Research Square

Preprints are preliminary reports that have not undergone peer review.
They should not be considered conclusive, used to inform clinical practice,
or referenced by the media as validated information.

Tartrazine–DNA Interaction Without Detectable Plasmid DNA Strand Cleavage: An Integrated Docking, Spectroscopic, Electrophoretic, and Antibacterial Study

ibrahim arman

ibrahimarmann@gmail.com

Bülent Ecevit University https://orcid.org/0000-0003-4603-7602

ismail Karakaya

Bülent Ecevit University https://orcid.org/0000-0002-8761-7841

Research Article

Keywords: tartrazine, azo food dye, antibacterial activityoxidative DNA damage, plasmid DNA cleavage, UV–Vis spectroscopy

Posted Date: September 23rd, 2026

DOI: https://doi.org/10.21203/rs.3.rs-11126206/v1

License: This work is licensed under a Creative Commons Attribution 4.0 International License.
Read Full License

Additional Declarations: The authors declare no competing interests.

Abstract

Tartrazine (E102) is one of the most widely used synthetic azo food colorants, yet its direct interaction with biomacromolecules and the biological relevance of these interactions remain incompletely understood. The present study investigated whether tartrazine binding to DNA is associated with structural DNA damage by integrating molecular docking, UV–Vis spectroscopy, plasmid DNA cleavage assays, and antibacterial susceptibility testing. Molecular docking predicted favorable binding of tartrazine to double-stranded DNA, with a binding free energy of − 7.00 kcal mol^{-1} and an estimated binding constant of 1.36×10^5 M^{-1}. UV–Vis spectrophotometric titration of calf thymus DNA showed a concentration-dependent hyperchromic effect without a significant shift in the absorption maximum. Benesi–Hildebrand analysis yielded an apparent DNA-binding constant on the order of 10^4 M^{-1} (reported as 3.88×10^4 M^{-1}) indicating a moderate binding affinity. Despite evidence of molecular interaction, agarose gel electrophoresis demonstrated that tartrazine did not induce detectable cleavage of pUC19 plasmid DNA under standard conditions. Likewise, tartrazine neither enhanced nor reduced oxidative DNA damage generated by the Fe^{2+}/H_2O_2 or Cu^{2+}/ascorbic acid systems within the tested concentration range. Antibacterial activity against Escherichia coli and Enterococcus faecalis was evaluated by broth microdilution and confirmed by colony-forming unit enumeration.No detectable growth-inhibitory effect was observed at the tested concentrations, and CFU enumeration did not indicate a reduction in viable bacterial counts.No detectable growth-inhibitory effect was observed at the tested concentrations. Collectively, these findings indicate that tartrazine is capable of interacting with DNA under cell-free conditions; however, this interaction was not accompanied by detectable plasmid DNA strand cleavage, modulation of oxidative DNA damage, or antibacterial activity. These results suggest that physicochemical binding alone should not be interpreted as evidence of direct genotoxicity.

Highlights

• Molecular docking predicted DNA-binding of tartrazine, a synthetic azo dye.

• UV–Vis titration showed spectral evidence of tartrazine binding to DNA.

• Tartrazine did not cleave pUC19 plasmid DNA under standard or oxidative conditions.

• Tartrazine showed no inhibitory effect on or growth.

• Biomolecular binding occurred without evidence of direct structural or antibacterial damage.

Introduction

Tartrazine (E102) is a synthetic, water-soluble azo dye widely used as a color additive in foods, pharmaceuticals, and cosmetic products. Its chemical structure contains azo and sulfonate functional groups that contribute to its high aqueous solubility and chemical stability (Rovina et al., 2017). Owing to its widespread consumption, tartrazine has been repeatedly evaluated by regulatory agencies, including

the European Food Safety Authority (EFSA) and the Joint FAO/WHO Expert Committee on Food Additives (JECFA). Although an acceptable daily intake has been established, concerns regarding its long-term biological safety remain, particularly with respect to potential genetic and oxidative effects (Aguilar et al., 2009; Amchova et al., 2024; Elhkim et al., 2007) .

The available literature presents inconsistent findings regarding the genotoxic potential of tartrazine. Several in vitro studies have reported chromosomal aberrations, micronucleus formation, or DNA strand damage following exposure to relatively high concentrations of the dye (Atlı Şekeroğlu et al., 2017; Ayub et al., 2007). In contrast, other investigations using human leukocytes, fibroblasts, and breast adenocarcinoma cells have detected little or no evidence of genotoxicity or cytotoxicity under comparable experimental conditions (Floriano et al., 2018; Merinas-Amo et al., 2019; Nasri & Pohjanvirta, 2021). Similarly, animal studies have produced conflicting results, with some reporting no detectable genotoxic effects, whereas others have associated prolonged exposure with oxidative stress and DNA damage (Bastaki et al., 2017; Khayyat et al., 2017). These discrepancies suggest that the biological effects of tartrazine depend strongly on the experimental model, exposure conditions, and biological context rather than reflecting an inherent DNA-damaging property.

Reactive oxygen species, particularly hydroxyl radicals generated through Fe^{2+}/H_2O_2- or Cu^{2+}/ascorbic acid-mediated reactions, are well-established mediators of oxidative DNA strand breakage (Halliwell & Gutteridge, 2015; Ozben, 1998). Because oxidative stress has been proposed as a potential mechanism underlying some reported toxicological effects of tartrazine (Khayyat et al., 2017), evaluating its behavior in these cell-free oxidative systems provides an opportunity to determine whether the compound directly influences DNA integrity in the absence of cellular metabolism and repair processes. Such experiments do not assess biological genotoxicity but instead examine the physicochemical interaction between tartrazine and DNA under controlled conditions.

Recent studies have also investigated the direct interaction of tartrazine with biomacromolecules. Spectroscopic and computational analyses have demonstrated that tartrazine is capable of interacting with double-stranded DNA, while spectroscopic studies have shown that the dye also binds serum albumin (S. Arsenault-Escobar et al., 2023; Pan et al., 2011). Although these studies provide evidence of molecular binding, they do not establish whether such interactions result in measurable structural DNA damage or alter biological function. Binding affinity alone cannot be interpreted as evidence of genotoxicity, making complementary functional assays necessary to evaluate the biological significance of these interactions.

To address this question, the present study combined molecular docking, UV–Vis spectrophotometric titration, and plasmid DNA electrophoresis under both standard and oxidative conditions to evaluate whether tartrazine binding is associated with detectable DNA strand damage. Antibacterial susceptibility assays against *Escherichia coli* and *Enterococcus faecalis* were also performed to determine whether the concentrations examined in the DNA-binding experiments were accompanied by measurable effects on bacterial growth. Together, these complementary approaches were used to assess whether

physicochemical interactions of tartrazine with DNA are associated with detectable structural DNA strand cleavage under the tested conditions or antibacterial activity under the experimental conditions employed.

Materials and Methods

2.1. Materials

pUC19 plasmid DNA (50 µg/mL working solution), a plasmid purification kit, ethanol, $FeSO_4$, H_2O_2, $CuSO_4$, $CaCl_2$, glycerol, ascorbic acid, TE (1×) buffer, tartrazine (granular form), calf thymus (CT) DNA, ethidium bromide, TAE (1×) buffer, agarose, and 6× loading dye (bromophenol blue, xylene cyanol, glycerol) were used. Antibacterial activity was assessed using Enterococcus faecalis ATCC 29212 and Escherichia coli ATCC 25922, obtained from the Department of Microbiology, Faculty of Medicine, Zonguldak Bülent Ecevit University. Tartrazine (analytical standard) and pUC19 plasmid DNA (D3404) were purchased from Sigma-Aldrich .

2.2. Direct DNA Cleavage Assay

The effect of tartrazine on pUC19 plasmid DNA integrity was evaluated following the method of Kitano et al. (Kitano et al., 2002). Reaction mixtures containing plasmid DNA (50 µg/mL in low-EDTA TE buffer) and tartrazine at final concentrations of 0, 0.936, 1.87, 2.80, 3.74, and 4.67 mM were prepared in reaction buffer (10 mM Tris-HCl, pH 7.4) to a constant final volume of 200 µL. The mixtures were incubated at 37 °C for 1 h and subsequently analyzed by electrophoresis on a 1% agarose gel containing an intercalating DNA stain. Electrophoresis was performed in 1× TAE buffer, and DNA bands were visualized using a gel documentation system. Untreated plasmid DNA served as the negative control. The relative distribution of the supercoiled (SC), open circular (OC), and linear (L) DNA forms was evaluated qualitatively by comparison of the electrophoretic band patterns.

2.3. Fenton-Mediated (Fe^{2+}/H_2O_2) Oxidative DNA Cleavage Assay

The effect of tartrazine on oxidative DNA damage induced by the Fe^{2+}/H_2O_2 (Fenton) system was evaluated according to the method of Kitano et al. (Kitano et al., 2002), with minor modifications. pUC19 plasmid DNA (50 µg/mL) was incubated with 15 mM $FeSO_4$ and 60 µM H_2O_2 at 37 °C for 1 h to generate hydroxyl radicals. Tartrazine was added at final concentrations of 0.936, 1.87, 2.80, 3.74, and 4.67 mM. A negative control containing plasmid DNA alone and a positive control containing DNA treated with $FeSO_4$ and H_2O_2 in the absence of tartrazine were included. All reaction mixtures were prepared in TE buffer (pH 7.4). Following incubation, DNA samples were separated by electrophoresis on a 1% agarose gel in 1× TAE buffer and visualized using a gel documentation system. The electrophoretic profiles were evaluated

qualitatively based on the relative distribution of the supercoiled (SC), open circular (OC), and linear (L) DNA conformations.

2.4. Effect of Tartrazine under Cu^{2+}/Ascorbic Acid-Induced Oxidative Conditions

The effect of tartrazine on Cu^{2+}/ascorbic acid-induced oxidative DNA damage was evaluated according to the method of Kitano et al.(Kitano et al., 2002). pUC19 plasmid DNA (50 µg/mL) was incubated with 60 µM $CuSO_4$ and 60 µM ascorbic acid at 37 °C for 1 h in the presence of tartrazine at final concentrations of 0.936, 1.87, 2.80, 3.74, and 4.67 mM. A negative control containing plasmid DNA alone was included, together with control reactions lacking either Cu^{2+} or ascorbic acid, as appropriate. All reaction mixtures were prepared in TE buffer (pH 7.4). Following incubation, DNA samples were resolved by electrophoresis on a 1% agarose gel in 1× TAE buffer at 90 V for 55 min. DNA bands corresponding to the supercoiled (SC), open circular (OC), and linear (L) conformations were visualized after ethidium bromide staining using a QUANTUM ST4 gel documentation system.

2.5. Spectroscopic Evidence of Tartrazine–DNA Interaction

The interaction between tartrazine and calf thymus DNA (ctDNA, 0.038 mM/ per base paire in 10mM low EDTA Tris buffer (pH 7.4)) was investigated by UV–Vis spectrophotometric titration according to the method of Arsenault-Escobar et al. (S. Arsenault-Escobar et al., 2023; Aslan et al., 2023). A 500 µL aliquot of ctDNA (0.038 mM) was kept constant throughout the experiment, while tartrazine (0.06 mM tartrazine in 10 mM low EDTA Tris buffer (, pH 7.4)) was added stepwise in 10 µL increments over ten titration steps. The total reaction volume was maintained constant after each addition. Absorbance spectra were recorded in the range of 200–400 nm following each titration step (5 min equilibration) using a UV–Vis spectrophotometer (Optizen 2120). Samples containing ctDNA alone and tartrazine alone were included as negative controls. To eliminate the contribution of the intrinsic absorbance of tartrazine, the absorbance values obtained for the tartrazine-only solutions at the corresponding concentrations were subtracted from those of the DNA–tartrazine mixtures prior to data analysis.

The apparent binding affinity between tartrazine and ctDNA was estimated using the Benesi–Hildebrand double-reciprocal equation:

$$1/(A - A_0) = 1/(A\infty - A_0) + 1/[K\square(A\infty - A_0)] \times 1/[\text{tartrazine}]$$

where A_0 is the absorbance of ctDNA at 260 nm in the absence of tartrazine, A is the absorbance measured after each addition of tartrazine, $A\infty$ is the absorbance at saturation, and Kb is the apparent DNA-binding constant. The binding constant was calculated from the slope and intercept of the linear regression obtained from the double-reciprocal.

2.6. Antibacterial Assays

Antibacterial activity was evaluated in LB broth using a broth microdilution assay. Bacterial cultures were grown overnight at 37 °C, and the medium was sterilized by autoclaving at 121 °C before use. The bacterial inocula were adjusted to an optical density of 0.1 at 600 nm (OD_{600}). Each well of a sterile 96-well microplate contained 50 µL of bacterial suspension, 100 µL of LB broth, and 50 µL of tartrazine solution, giving a final reaction volume of 200 µL and final tartrazine concentrations of 0 (control), 33, 111, 333, 1000, and 3000 µg/mL. *Escherichia coli* and *Enterococcus faecalis* were tested in parallel under identical experimental conditions. The initial OD_{600} was recorded using a microplate reader (Thermo Scientific™ Multiskan™ Sky), after which the plates were incubated at 37 °C for 24 h in a shaking incubator. Following incubation, bacterial growth was evaluated by measuring OD_{600} again using the same microplate reader (Wiegand et al., 2008).

Antibacterial activity was further confirmed by colony-forming unit (CFU) analysis. Aliquots from each treatment group were spread onto LB agar plates and incubated at 37 °C for 24 h, after which viable colonies were counted to assess bacterial survival. Each concentration was tested in triplicate. All experiments were performed independently three times, and the data are presented as the mean ± standard deviation (SD).

2.7. Molecular Docking

The three-dimensional crystal structure of B-form double-stranded DNA (PDB ID: 1BNA; resolution 1.90 Å) was retrieved from the RCSB Protein Data Bank. The three-dimensional structure of tartrazine (PubChem CID: 5281871) was obtained from the PubChem database in SDF format. The DNA structure was prepared by removing crystallographic water molecules and non-essential ions using BIOVIA Discovery Studio Visualizer (v21). The ligand structure was converted to the appropriate format and prepared for molecular docking.

Prior to docking, both the DNA receptor and the tartrazine ligand were energy-minimized using the molecular mechanics force field implemented in Avogadro (v1.2.0) to optimize bond lengths, bond angles, and torsional conformations. The minimized structures were subsequently prepared using AutoDockTools (ADT, v1.5.7) by adding polar hydrogen atoms and assigning Gasteiger charges.

Molecular docking simulations were carried out using AutoDock Vina (v1.2.7). The docking grid was centered at x = 14.779, y = 21.144, z = 9.521, with dimensions of 24 × 28 × 46 and a grid spacing of 1.0 Å, covering the entire DNA binding region. Ten independent docking runs were performed, and the resulting poses were ranked according to their predicted binding free energies. The conformation exhibiting the lowest binding free energy was selected as the most favorable binding mode for subsequent analyses. DNA–ligand interactions, including hydrogen bonding and hydrophobic contacts, were analyzed and visualized using BIOVIA Discovery Studio Visualizer (v21) and UCSF Chimera (v1.16) (Aslan et al., 2023; Gumus & Arman, 2021).

2.8. Statistical Analysis

All quantitative experiments were performed independently at least three times, and data are expressed as the mean ± standard deviation (SD). Statistical analyses were performed using GraphPad Prism version 10.0 (GraphPad Software, San Diego, CA, USA). For quantitative datasets, including antibacterial growth measurements, differences among groups were evaluated by one-way analysis of variance (ANOVA) followed by Dunnett's multiple comparisons test using the untreated control as the reference group. A value of $P < 0.05$ was considered statistically significant. Spectroscopic binding analyses were evaluated by linear regression, and the goodness of fit was assessed using the coefficient of determination (R^2). DNA cleavage assays were interpreted qualitatively based on agarose gel electrophoretic band patterns.

Results

3.1. Docking-Predicted Binding Mode of Tartrazine on Double-Stranded DNA

Molecular docking predicted that tartrazine binds favorably to double-stranded DNA with a binding free energy of − 7.00 kcal/mol, corresponding to an estimated binding constant (Kb) of 1.36×10^5 M^{-1}. The lowest-energy docking pose positioned tartrazine between adjacent DNA base pairs, suggesting an intercalative binding orientation. Analysis of the interaction profile revealed hydrogen bonds with nucleotides dC21(B), dG22(B), and dG24(B), with predicted bond distances ranging from 2.8 to 3.0 Å. In addition, hydrophobic interactions, including π–π stacking contacts, were observed between the aromatic rings of tartrazine and nucleotides dG2(A), dC3(A), and dG4(A). These interactions are consistent with a favorable predicted association between tartrazine and double-stranded DNA (Fig. 1).

3.2. Spectroscopic Evidence of Tartrazine–DNA Interaction

UV–Vis absorption spectroscopy revealed a concentration-dependent increase in the absorbance of calf thymus DNA following the addition of tartrazine, resulting in a distinct hyperchromic effect without a significant shift in the absorption maximum (Fig. 2). The observed hyperchromic effect is consistent with an interaction between tartrazine and DNA and may reflect changes in the local environment of DNA chromophores.

The DNA-binding affinity was quantified using the Benesi–Hildebrand double-reciprocal method. Linear regression analysis produced the equation $y = 0.0003x + 3.88$, with a correlation coefficient of $R^2 = 0.9884$. The apparent DNA-binding constant (Kb) was calculated as 3.88×10^4 M^{-1}, corresponding to a binding free energy of − 6.25 kcal mol^{-1}. This binding constant is considerably lower than those typically reported for classical DNA intercalators indicating a moderate affinity between tartrazine and DNA.

The docking analysis (Section 3.1) identified a base-pair-associated pose as the lowest-energy predicted orientation. The spectroscopic data were consistent with a non-covalent tartrazine–DNA interaction but did not distinguish between intercalative and groove-associated binding geometries.

3.3. Effect of Tartrazine Alone on pUC19 Plasmid DNA Integrity

The direct DNA cleavage assay demonstrated that tartrazine did not induce detectable structural damage to pUC19 plasmid DNA at any of the tested concentrations (0.936–4.67 mM) (Fig. 3). In all treatment groups, the supercoiled (SC) plasmid remained the predominant DNA conformer, while the open circular (OC) band showed no apparent increase compared with the untreated control. No linear (L) DNA band was observed in any lane, indicating the absence of double-strand DNA cleavage. The electrophoretic profiles obtained after tartrazine treatment were essentially indistinguishable from those of the untreated control, indicating that no detectable plasmid-cleaving activity was observed under the experimental conditions employed.

3.4. Effect of Tartrazine under Fe^{2+}/H_2O_2-Induced Oxidative Conditions

Exposure of pUC19 plasmid DNA to the Fe^{2+}/H_2O_2 system resulted in extensive oxidative DNA damage, evidenced by the marked loss of the supercoiled (SC) DNA band and the predominance of slower-migrating DNA species. In the presence of tartrazine (0.936–4.67 mM), the electrophoretic pattern remained comparable to that of the positive control, with no restoration of the supercoiled DNA band observed. Increasing the tartrazine concentration did not noticeably alter the extent of oxidative DNA damage induced by the Fenton reaction. No detectable protective or enhancing effect of tartrazine on Fe^{2+}/H_2O_2-induced plasmid DNA damage was observed under the tested conditions.

3.5. Effect of Tartrazine under Cu^{2+}/Ascorbic Acid-Induced Oxidative Conditions

The Cu^{2+}/ascorbic acid system induced extensive oxidative damage to pUC19 plasmid DNA, evidenced by the marked loss of the supercoiled (SC) DNA band compared with the untreated control (Fig. 5). Addition of tartrazine at concentrations ranging from 0.936 to 4.67 mM did not visibly alter the electrophoretic pattern produced by the Cu^{2+}/ascorbic acid system, with no visually apparent protective effect across the tested tartrazine concentrations. Control reactions further demonstrated that Cu^{2+} alone did not induce appreciable DNA damage, and tartrazine alone (4.67 mM) did not exhibit intrinsic DNA cleavage activity. Overall, these findings indicate that tartrazine neither protected against nor enhanced Cu^{2+}/ascorbic acid-mediated oxidative DNA damage under the experimental conditions employed.

3.6. Effect of Tartrazine on the Growth of *E. coli* and *E. faecalis*

The antibacterial activity of tartrazine against Escherichia coli and Enterococcus faecalis was evaluated by broth microdilution and confirmed by colony-forming unit (CFU) enumeration (Fig. 6). One-way ANOVA revealed a significant overall effect of tartrazine concentration on bacterial growth in both E. coli ($F(5,12) = 12.16$, $P = 0.0002$) and E. faecalis ($F(5,12) = 17.83$, $P < 0.0001$). Brown–Forsythe tests detected no significant evidence of heterogeneity of variances for both species (E. coli: $P = 0.5411$; E. faecalis: $P = 0.5909$).

For *E. coli*, Dunnett's multiple comparison test showed no significant differences in relative growth at 33 or 111 µg/mL compared with the untreated control ($P = 0.3804$ and 0.2357, respectively). However, bacterial growth increased significantly at 333, 1000, and 3000 µg/mL (adjusted $P = 0.0091$, 0.0042, and < 0.0001, respectively), reaching 128.9%, 132.2%, and 152.5% of the control. Similarly, *E. faecalis* exhibited no significant change in growth at 33, 111, or 333 µg/mL (adjusted $P = 0.9825$, 0.9994, and 0.1856, respectively), whereas significant increases were observed at 1000 and 3000 µg/mL (adjusted $P = 0.0036$ and < 0.0001), corresponding to 116.8% and 127.0% of the untreated control.

CFU enumeration was consistent with the OD_{600} measurements and did not indicate a reduction in viable bacterial counts at the tested concentrations. Collectively, these findings indicate that tartrazine did not inhibit the growth of either bacterial species under the experimental conditions and, at higher concentrations, was associated with a significant increase in bacterial growth.

Discussion

The molecular docking analysis predicted that tartrazine can associate with double-stranded DNA through energetically favorable non-covalent interactions. The lowest-energy docking pose suggested that the ligand occupies a position between adjacent base pairs while simultaneously forming hydrogen bonds and hydrophobic contacts with neighboring nucleotides. Although these interactions indicate that tartrazine is structurally compatible with DNA, docking provides only a computational prediction of a possible binding mode and should not be considered direct evidence of molecular recognition under physiological conditions. As docking simulations are performed using a static receptor model, they do not account for DNA flexibility, solvent effects, ionic strength, or other dynamic factors that may influence ligand binding in solution (S. Arsenault-Escobar et al., 2023) .

The UV–Vis titration experiments independently demonstrated that tartrazine interacts with calf thymus DNA in solution. Progressive addition of tartrazine produced a concentration-dependent hyperchromic effect without a measurable shift in the absorption maximum, indicating that the interaction altered the local environment of the DNA chromophores while preserving the overall spectral profile. The calculated binding constant ($K_b = 3.88 \times 10^4\ M^{-1}$) supports a measurable interaction between tartrazine and DNA. However, the magnitude of K_b alone is insufficient to distinguish between different DNA-binding mode.

This value is of the same order of magnitude as binding constants reported for other azo food colorants that interact with DNA through a groove-binding mode, such as carmoisine ($K_b \approx 10^4\ M^{-1}$; Basu & Kumar, 2014), and for tartrazine itself in an independent study combining UV–vis and electrochemical titration ($K_b = 4.45 \times 10^4–5.75 \times 10^4\ M^{-1}$) (S Arsenault-Escobar et al., 2023). Classical intercalators such as ethidium bromide and acridine orange have also been reported with binding constants in a broadly comparable range ($K_b \approx 2.7 \times 10^4–6.6 \times 10^4\ M^{-1}$) (Nafisi et al., 2007), indicating that the magnitude of K_b alone cannot be used to infer the binding mode of tartrazine; complementary structural evidence is required for that purpose.

The docking analysis and the spectroscopic titration probe different aspects of ligand–DNA interaction and are not expected to yield identical descriptors of binding geometry. Molecular docking identifies a geometrically favorable pose under static, computational conditions, whereas UV–Vis spectroscopy reports the averaged behavior of the ligand population in solution. The spectroscopic data (hyperchromism without a shift in absorption maximum) are consistent with a non-covalent interaction but do not, on their own, confirm or exclude classical intercalation, nor do they exclude the possibility that multiple weak binding orientations coexist in solution. Taken together, the docking-predicted base-pair-associated pose and the spectroscopic evidence of a moderate-affinity, non-covalent interaction are compatible with - but do not independently establish - a groove-binding or other non-classical-intercalative mode - consistent with the minor-groove binding mode reported for tartrazine itself on the basis of QM/MM calculations (Arsenault-Escobar et al., 2023) and with the groove-binding behavior described for the structurally related azo colorant carmoisine (Basu & Kumar, 2014); this should be regarded as a working hypothesis rather than a demonstrated binding geometry.

The present observations are generally consistent with the study of Arsenault-Escobar et al. (2023), who also reported direct interaction between tartrazine and double-stranded DNA using spectroscopic and electrochemical approaches, identifying a minor-groove binding mode through combined UV–vis, electrochemical, and QM/MM analysis, with binding constants ($4.45 \times 10^4–5.75 \times 10^4\ M^{-1}$) close to the value obtained in the present study. The current work extends those observations by combining computational prediction with spectroscopic analysis and subsequently examining whether the detected interaction is associated with structural DNA damage. This experimental design allows molecular interaction to be evaluated separately from detectable plasmid DNA cleavage and bacterial growth effects.

Although molecular docking and UV–Vis spectroscopy demonstrated that tartrazine is capable of interacting with DNA, these interactions were not accompanied by detectable structural damage in the plasmid DNA cleavage assay. Under the experimental conditions employed, tartrazine alone neither converted the supercoiled plasmid into the open circular or linear forms nor produced evidence of strand cleavage. These findings indicate that the tartrazine–DNA interaction observed in the present study was not accompanied by detectable plasmid DNA strand cleavage under the tested cell-free conditions. This distinction is important because molecular association and genotoxicity represent different biological endpoints and should not be considered interchangeable.

The absence of detectable plasmid DNA cleavage is broadly compatible with studies reporting no measurable genotoxic effects under specific experimental conditions (Bastaki et al., 2017; Floriano et al., 2018; Merinas-Amo et al., 2019; Nasri & Pohjanvirta, 2021). At the same time, it differs from studies reporting DNA damage in mammalian cells or experimental animals following tartrazine exposure (Atlı Şekeroğlu et al., 2017; Khayyat et al., 2017; Soares et al., 2015). Direct comparison between these studies should be made with caution because they differ substantially in experimental model, biological endpoint, exposure conditions, and the presence of cellular metabolism. The present work was performed using purified plasmid DNA in a cell-free system and therefore evaluates only the intrinsic ability of tartrazine to damage DNA directly; it does not address mechanisms that depend on cellular uptake, metabolic transformation, DNA repair, or intracellular oxidative stress.

To further investigate whether oxidative conditions modify the effect of tartrazine on DNA integrity, plasmid DNA was exposed to two independent radical-generating systems, Fe^{2+}/H_2O_2 and Cu^{2+}/ascorbic acid. In both assays, oxidative DNA damage was readily produced by the oxidizing systems themselves, whereas the addition of tartrazine did not visibly alter the electrophoretic pattern relative to the corresponding positive controls. Within the concentration range examined, these observations provide no evidence that tartrazine either enhanced or inhibited oxidative plasmid DNA strand cleavage under the experimental conditions used. This is noteworthy because classical DNA intercalators are known to protect plasmid DNA against Fenton-type oxidative strand cleavage, an effect attributed to local conformational changes and unwinding of the duplex at the intercalation site that limit hydroxyl-radical access to the deoxyribose backbone (Kim et al., 2014). The absence of a comparable protective effect for tartrazine in the present study is compatible with a non-intercalative binding mode, although this observation alone does not exclude intercalation, since the protective effect described by Kim et al. (Kim et al., 2014) was dependent on intercalator concentration and the ligand-to-DNA ratio.

These findings should be interpreted within the limitations of the experimental model. Agarose gel electrophoresis provides a reliable qualitative assessment of changes in plasmid topology but is less sensitive than quantitative approaches for detecting subtle differences in oxidative DNA damage. Accordingly, the present data support the conclusion that no obvious concentration-dependent effect of tartrazine was observed in either oxidative system, but they cannot exclude the possibility of smaller effects that might become detectable using more sensitive quantitative assays. The present results therefore do not support a direct role for tartrazine in promoting oxidative plasmid DNA strand cleavage under the conditions examined, while they also do not exclude mechanisms that may operate in more complex cellular environments.

Overall, the DNA cleavage experiments complement the docking and spectroscopic findings by demonstrating that measurable DNA binding does not necessarily translate into detectable structural DNA damage. Within the limitations of a purified plasmid model, the results consistently indicate that tartrazine binds DNA without producing direct strand cleavage, either under basal conditions or in the presence of the Fe^{2+}/H_2O_2 and Cu^{2+}/ascorbic acid oxidative systems investigated in this study.

The antibacterial assays demonstrated that tartrazine did not inhibit the growth of either Escherichia coli or Enterococcus faecalis within the concentration range investigated. Relative bacterial growth remained comparable to or higher than that of the untreated control, and CFU enumeration was consistent with the spectrophotometric measurements, providing no evidence of detectable growth-inhibitory activity under the experimental conditions employed. The agreement between OD_{600} measurements and CFU analysis provides complementary evidence regarding bacterial growth and viable colony counts at the concentrations tested.

The present findings are consistent with previous bacterial mutagenicity studies in which tartrazine did not show mutagenic activity in standard *Salmonella typhimurium* tester strains, with or without metabolic activation (Izbirak et al., 1990). Although bacterial mutagenicity assays and antibacterial susceptibility tests address different biological endpoints, the absence of mutagenic activity reported in previous studies is not inconsistent with the lack of growth inhibition observed in the present study.

An increase in relative bacterial growth was observed at higher tartrazine concentrations. However, the present data do not permit determination of the underlying mechanism responsible for this observation. Because the study was designed to evaluate antibacterial activity rather than bacterial metabolism or nutrient utilization, it cannot distinguish whether the increased optical density reflects enhanced bacterial proliferation, changes in culture turbidity, or other experimental factors. Azo dyes have been reported to support bacterial growth as an auxiliary carbon and nitrogen source under certain culture conditions (Chang & Kuo, 2000), which represents one of several possible, but currently unconfirmed, explanations for the present observation. Any mechanistic interpretation of the observed increase would be speculative and is beyond the scope of the present study.

Overall, the antibacterial assays indicate that tartrazine did not produce detectable growth-inhibitory activity against the tested E. coli and E. faecalis strains under the experimental conditions employed. These findings complement the DNA-binding and DNA cleavage experiments by showing that, despite measurable biomolecular interactions with DNA observed in vitro, tartrazine did not produce detectable antibacterial effects in the bacterial models used in this study.

This study has several limitations. All DNA-binding and DNA cleavage experiments were performed using purified biomolecules in cell-free systems, which do not fully represent the complexity of cellular or in vivo environments. In addition, although molecular docking and UV–Vis spectroscopy consistently supported DNA binding, these methods alone cannot definitively establish the binding mode. Further structural studies, such as circular dichroism spectroscopy or molecular dynamics simulations, would help to characterize the interaction in greater detail. Such approaches have previously helped resolve the binding mode of structurally related DNA-interacting dyes — for example, circular dichroism and dye-displacement titrations were used to confirm minor-groove binding for carmoisine (Basu & Suresh Kumar, 2014), and QM/MM-based computational modeling was used to define the tartrazine–DNA binding mode at atomic resolution (S Arsenault-Escobar et al., 2023). Oxidative DNA damage was assessed qualitatively by agarose gel electrophoresis, which may not detect subtle changes in DNA

integrity. Finally, the antibacterial activity was evaluated using only two reference bacterial strains, limiting the generalizability of these findings to other microorganisms.

Despite these limitations, the results consistently indicate that tartrazine binds to DNA without causing detectable plasmid DNA strand cleavage under the experimental conditions used. Future studies employing complementary cellular models and structural approaches will help clarify the biological significance of this interaction.

Conclusion

This study investigated the interaction of tartrazine with DNA using complementary computational, spectroscopic, electrophoretic, and antibacterial approaches. Molecular docking predicted a favorable association of tartrazine with double-stranded DNA, while UV–Vis spectrophotometric titration provided evidence consistent with a measurable interaction between tartrazine and calf thymus DNA. The apparent DNA-binding constant obtained from Benesi–Hildebrand analysis was $3.88 \times 10^4\ M^{-1}$. However, the spectroscopic and docking results did not establish a specific DNA-binding mode.

Despite the observed DNA interaction, tartrazine did not produce detectable plasmid DNA strand cleavage under the tested conditions. Similarly, no detectable enhancement or inhibition of oxidative plasmid DNA damage was observed in the Fe^{2+}/H_2O_2 and Cu^{2+}/ascorbic acid systems within the tested concentration range.

Tartrazine also did not produce detectable growth-inhibitory activity against the tested Escherichia coli and Enterococcus faecalis strains within the concentration range examined. Together, these findings indicate that the tartrazine–DNA interaction observed under the present cell-free conditions was not accompanied by detectable plasmid DNA strand cleavage or growth-inhibitory activity against the bacterial strains examined.

The findings also emphasize that a physicochemical interaction with DNA should not, by itself, be interpreted as evidence of DNA damage or genotoxicity. Because the present experiments used purified DNA and only two bacterial strains under defined experimental conditions, the findings should not be extrapolated directly to mammalian cells or in vivo systems. Further studies using complementary structural and cellular approaches are needed to determine whether tartrazine–DNA interactions have functional consequences under more physiologically relevant conditions.

Declarations

6. Author Contributions

İbrahim Arman: Conceptualization, Methodology, Project administration, Supervision, Writing – original draft, Writing – review & editing. İsmail Karakaya: Investigation, Methodology. All authors reviewed and approved the final version of the manuscript.

7. Conflict of Interest / Disclosure Statement

The authors declare that they have no known competing financial interests or personal relationships that could have appeared to influence the work reported in this manuscript.

8. Funding

This work was supported by the Scientific Research Projects Coordination Unit of Zonguldak Bülent Ecevit University under Project No. 2023-50737594-01

9. Data Availability Statement

The data generated and analyzed during the current study are available from the corresponding author upon reasonable request.

10. Ethics Statement

No ethical approval was required for this study because it did not involve human participants, human-derived clinical samples, or experimental animals.

References

1. Aguilar F, Charrondiere U, Dusemund B, Galtier P, Gilbert J, Gott D, Lambré C (2009) Scientific opinion on the re-evaluation Tartrazine (E 102). EFSA J 1331:1–52
2. Amchova P, Siska F, Ruda-Kucerova J (2024) Safety of tartrazine in the food industry and potential protective factors. Heliyon, 10(18), e38111
3. Arsenault-Escobar S, Fuentes-Galvez J, Orellana C, Bollo S, Sierra–Rosales P, Miranda-Rojas S (2023) Unveiling the tartrazine binding mode with ds–DNA by UV–visible spectroscopy, electrochemical, and QM/MM methods. Spectrochim Acta Part A Mol Biomol Spectrosc 292:122400
4. Arsenault-Escobar S, Fuentes-Galvez JF, Orellana C, Bollo S, Sierra-Rosales P, Miranda-Rojas S (2023) Unveiling the tartrazine binding mode with ds-DNA by UV-visible spectroscopy, electrochemical, and QM/MM methods. Spectrochim Acta Part A Mol Biomol Spectrosc 292:122400
5. Aslan C, Arman I, Nabi-Afjadi M, Zalpoor H (2023) Evaluation of dexamethasone and its combination with mineral supplements on the DNA compactness/breakage and the efficiency of antioxidant defense enzymes. Toxicol Environ Health Sci 15(3):207–215
6. Atlı Şekeroğlu Z, Sönmez D, Karakaya S (2017) Genotoxic effects of tartrazine on human peripheral lymphocytes in vitro. Cytotechnology 69(3):407–414
7. Ayub AC, Gomes AD, Lima MV, Vianna-Soares CD, Ferreira LA (2007) Topical delivery of fluconazole: in vitro skin penetration and permeation using emulsions as dosage forms. Drug Dev Ind Pharm 33(3):273–280

8. Bastaki M, Farrell T, Bhusari S, Pant K, Lackner K (2017) Lack of genotoxicity in vivo for food color additive tartrazine. Food Chem Toxicol 105:278–284
9. Basu A, Suresh Kumar G (2014) Minor groove binding of the food colorant carmoisine to DNA: Spectroscopic and calorimetric characterization studies. J Agric Food Chem 62(1):317–326
10. Elhkim MO, Héraud F, Bemrah N, Gauchard F, Lorino T, Lambré C, Poul JM (2007) New considerations regarding the risk assessment on tartrazine. Regul Toxicol Pharmacol 47(3):308–316
11. Floriano JF, Silva DF, da Costa FB, Varanda EA (2018) Evaluation of tartrazine-induced DNA damage in human leukocytes ex vivo. Mutat Research/Genetic Toxicol Environ Mutagen 829–830:19–23
12. Gumus GK, Arman I (2021) Effect of verapamil on Enterococcus faecalis, Escherichia coli and on DNA damage induced by copper and iron. Indian J Experimental Biology (IJEB) 59(11):791–797
13. Halliwell B, Gutteridge JMC (2015) Free radicals in biology and medicine, 5th edn. ed.): Oxford University Press
14. Izbirak A, Sümer S, Diril N (1990) Mutagenicity testing of some azo dyes used as food additives. Mikrobiyoloji Bulteni 24(1):48–56
15. Khayyat LI, Essawy AE, Sorour JM, Soffar A, El-Gohary A (2017) Tartrazine induces oxidative stress and DNA damage. Toxicol Rep 4:398–404
16. Kim HJ, Sung G, Kim G, Park J, Jin B, Kim SK (2014) Effect of Various Intercalators on the Fenton-Type Oxidative Cleavage of Double-Stranded DNA. Chemistry–An Asian J 9(5):1341–1348
17. Kitano K, Fukukawa T, Ohtsuji Y, Masuda T, Yamaguchi H (2002) DNA-damaging activity caused by decomposed potassium sorbate. Food Chem Toxicol 40(11):1589–1594
18. Merinas-Amo R, Alonso-Moraga A, Calahorra J, Muñoz-Serrano A (2019) Genotoxicity testing of tartrazine. Food Chem Toxicol 131:110529
19. Nafisi S, Saboury AA, Keramat N, Neault J-F, Tajmir-Riahi H-A (2007) Stability and structural features of DNA intercalation with ethidium bromide, acridine orange and methylene blue. J Mol Struct 827(1–3):35–43
20. Nasri H, Pohjanvirta R (2021) Lack of genotoxicity of tartrazine in MCF-7 cells. Toxicol In Vitro 75:105192
21. Ozben T (1998) Free radicals, oxidative stress, and antioxidants. Springer
22. Pan X, Qin P, Liu R, Wang J (2011) Characterizing the interaction between tartrazine and two serum albumins. J Agric Food Chem 59(12):6650–6656
23. Rovina K, Siddiquee S, Shaarani SM (2017) Determination of tartrazine in foodstuffs. Crit Rev Anal Chem 47(4):309–324
24. Soares BM, de Oliveira DN, Santos VC, Justino GC (2015) DNA damage in lymphocytes exposed to tartrazine. Food Chem Toxicol 78:123–129
25. Wiegand I, Hilpert K, Hancock RE (2008) Agar and broth dilution methods to determine the minimal inhibitory concentration (MIC) of antimicrobial substances. Nat Protoc 3(2):163–175

Figures

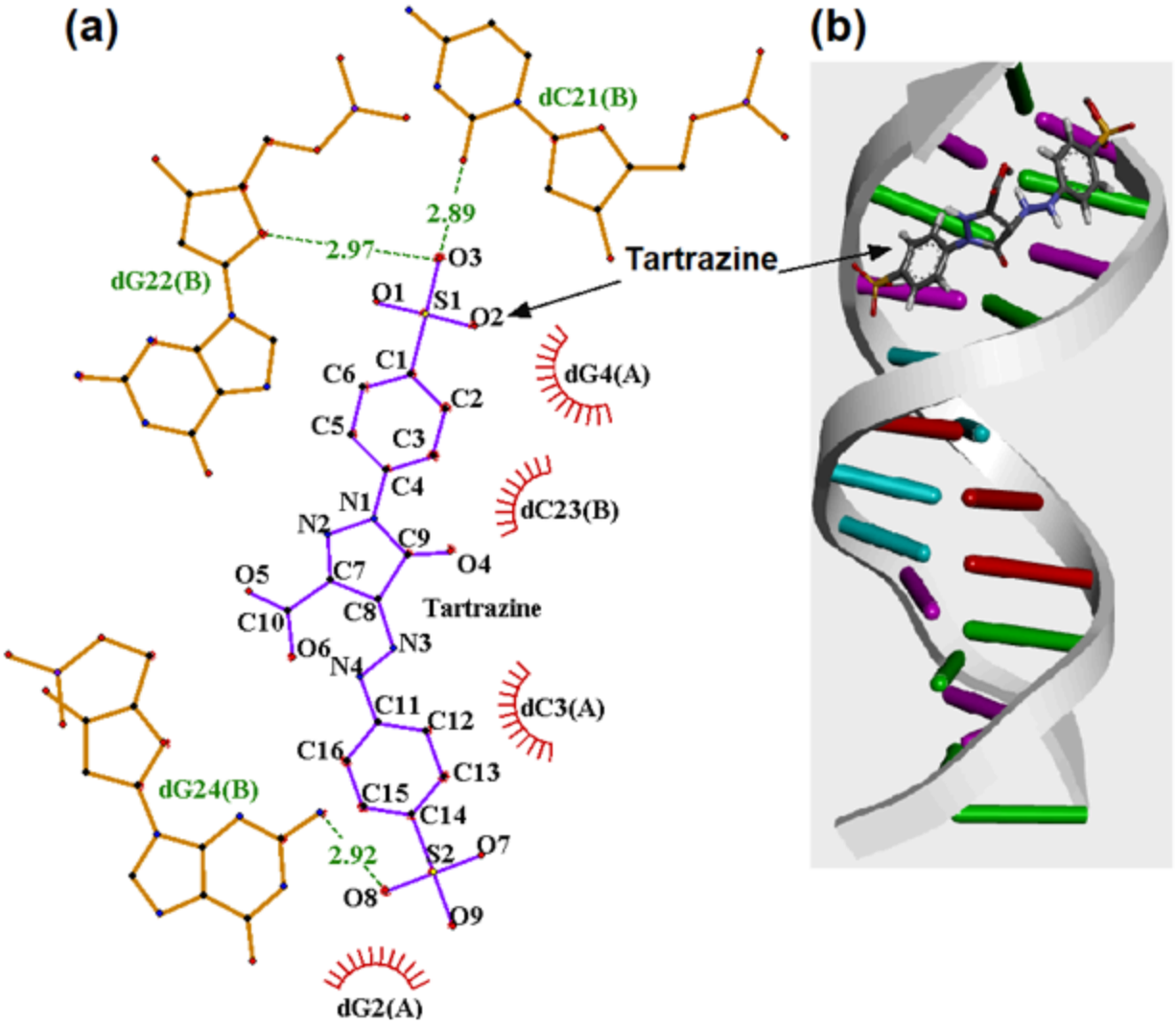


Figure 1

Molecular docking analysis of tartrazine with double-stranded DNA (PDB ID: 1BNA). (A) Predicted three-dimensional binding pose of tartrazine within the DNA duplex, showing its intercalative orientation between adjacent base pairs. (B) Two-dimensional interaction diagram illustrating the hydrogen bonds formed with nucleotides dC21(B), dG22(B), and dG24(B), together with hydrophobic and π–π stacking interactions involving dG2(A), dC3(A), and dG4(A). The lowest-energy docking pose exhibited a binding free energy of −7.00 kcal/mol, corresponding to an estimated binding constant (Kb) of $1.36 \times 10^5\ M^{-1}$.

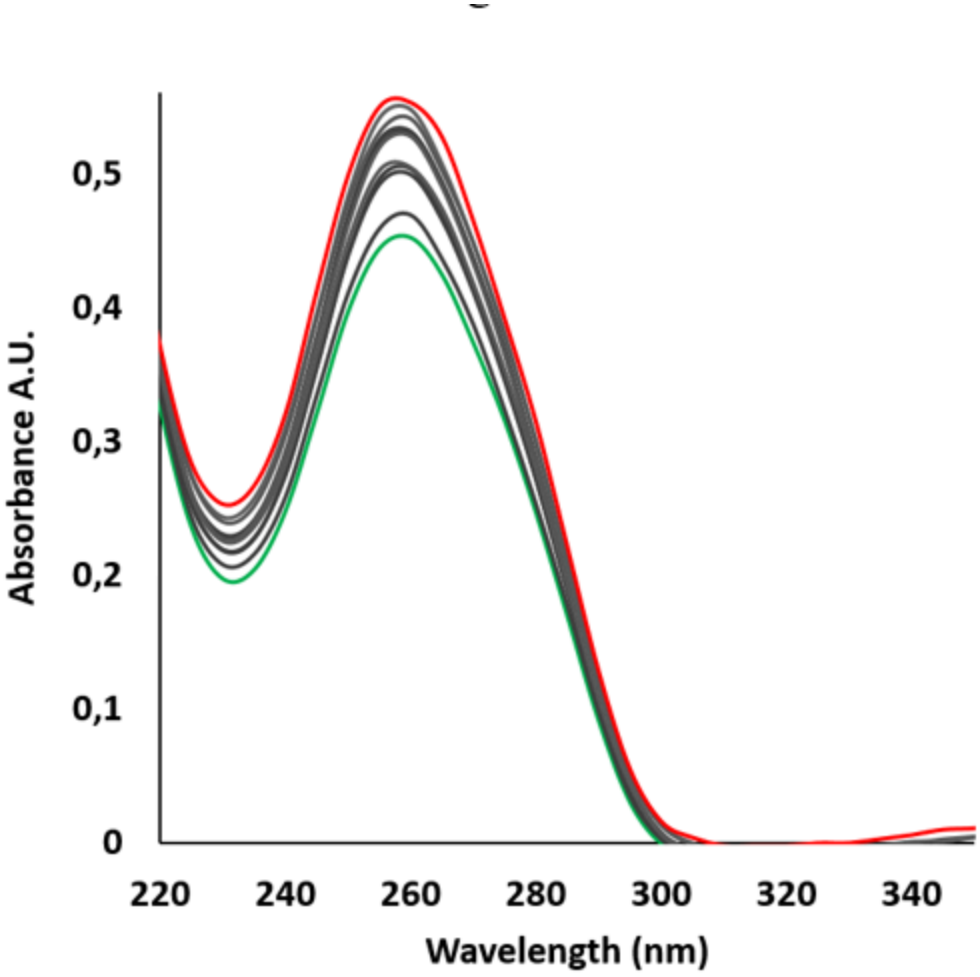


Figure 2

UV–Vis absorption spectra of calf thymus DNA following stepwise titration with tartrazine. The concentration of calf thymus DNA was kept constant throughout the experiment, whereas tartrazine (0.06 mM) was added in ten successive 10 µL increments. Absorbance spectra were recorded over the wavelength range of 200–400 nm after each addition. Spectra were corrected by subtracting the absorbance of tartrazine-only solutions at the corresponding concentrations to eliminate the intrinsic absorbance of the ligand. The progressive increase in absorbance at the DNA absorption band was used for subsequent Benesi–Hildebrand analysis to determine the apparent DNA-binding constant.

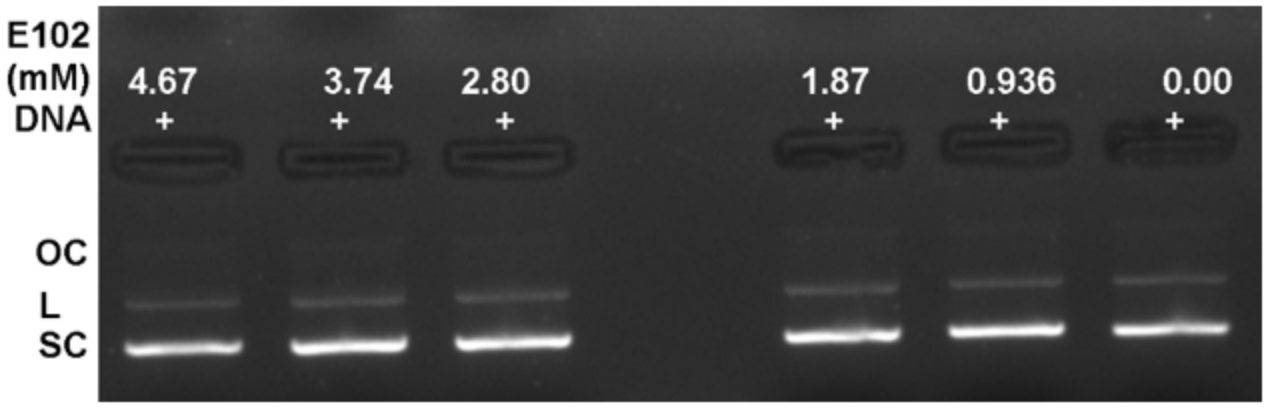


Figure 3

Direct DNA cleavage assay of pUC19 plasmid DNA following incubation with increasing concentrations of tartrazine. Lane M, DNA molecular weight marker; Lane 1, untreated control; Lanes 2–6, plasmid DNA treated with tartrazine (0.936–4.67 mM). DNA was resolved on a 1% agarose gel. SC, supercoiled DNA; OC, open circular DNA. No detectable DNA strand cleavage was observed at any tested concentration.

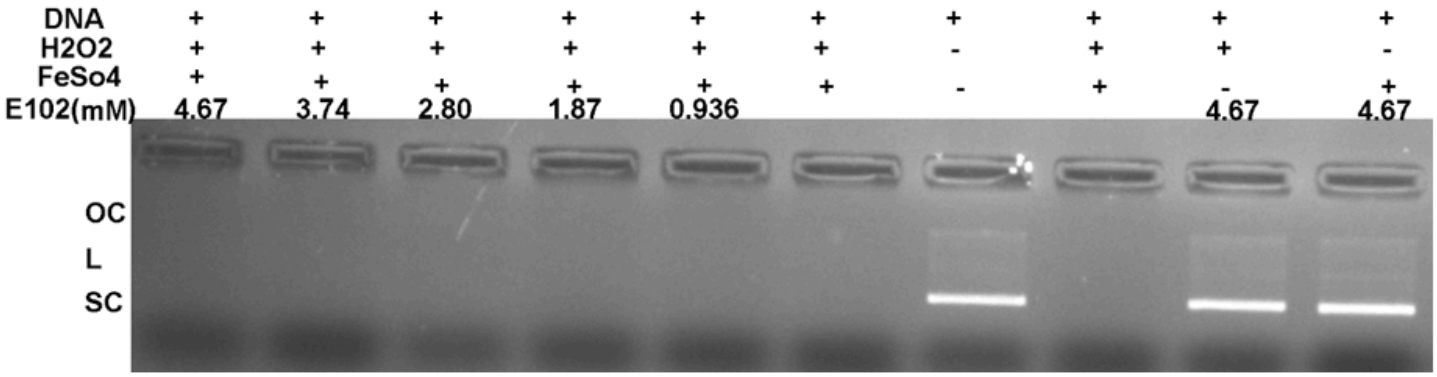


Figure 4

Effect of tartrazine on Fe^{2+}/H_2O_2-induced oxidative cleavage of pUC19 plasmid DNA. Plasmid DNA (50 µg/mL) was incubated with $FeSO_4$ (15 mM) and H_2O_2 (60 µM) in the absence or presence of tartrazine (0.936–4.67 mM), as indicated. DNA samples were separated on a 1% agarose gel. Lanes 1–5: DNA + Fe^{2+} + H_2O_2 containing 4.67, 3.74, 2.80, 1.87, and 0.936 mM tartrazine, respectively. Lane 6 and 8: positive control (DNA + Fe^{2+} + H_2O_2, without tartrazine). Lane 7: negative control (DNA alone). Lane 9: DNA + H_2O_2 + tartrazine (4.67 mM). lane 10 : DNA + $FeSO_4$ + tartrazine (4.67 mM) . The symbols (+) and (−) indicate the presence and absence, respectively, of plasmid DNA, $FeSO_4$, H_2O_2, and tartrazine in each reaction mixture. SC, supercoiled DNA; OC, open circular DNA; L, linear DNA.

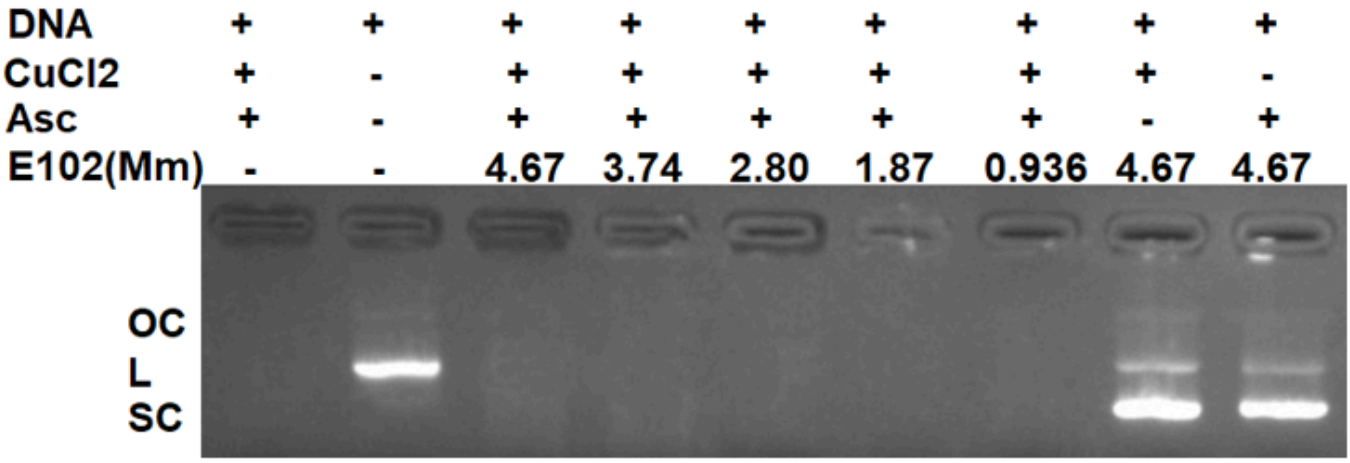


Figure 5

Effect of tartrazine on Cu^{2+}/ascorbic acid-induced oxidative cleavage of pUC19 plasmid DNA. Plasmid DNA (50 µg/mL) was incubated with 60 µM $CuSO_4$ and 60 µM ascorbic acid in the absence or presence of tartrazine (0.936–4.67 mM). DNA samples were separated on a 1% agarose gel (90 V, 55 min) and visualized after ethidium bromide staining. Lane 1, Cu^{2+}/ascorbic acid-treated DNA (positive control); Lane 2, untreated DNA (negative control); Lanes 3–7, Cu^{2+}/ascorbic acid-treated DNA containing 4.67, 3.74, 2.80, 1.87, and 0.936 mM tartrazine, respectively; Lane 8, DNA incubated with Cu^{2+} and 4.67 mM tartrazine ; Lane 9, DNA incubated with Aschorbic acidAscorbic acid and 4.67 mM tartrazine. The symbols (+) and (−) indicate the presence and absence, respectively, of plasmid DNA, $CuSO_4$, H_2O_2, and tartrazine in each reaction mixture . SC, supercoiled DNA; OC, open circular DNA; L, linear DNA.

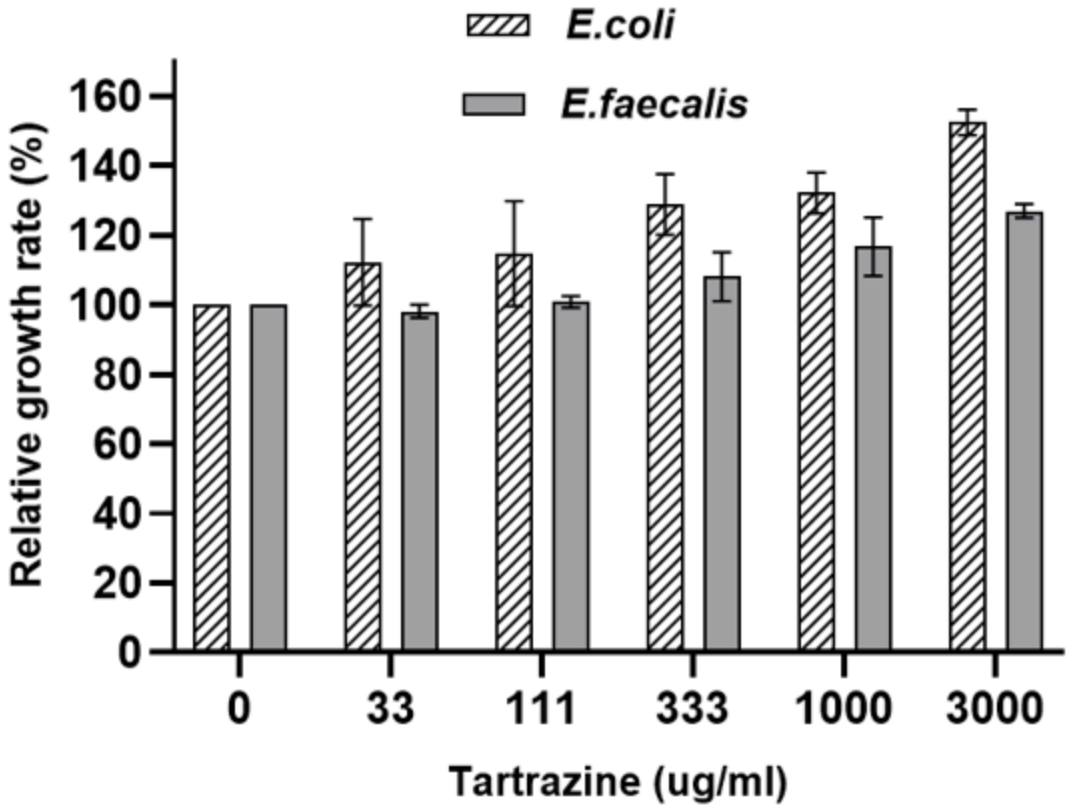


Figure 6

Effect of tartrazine on the growth of *Escherichia coli* and *Enterococcus faecalis*. Relative bacterial growth was determined from the optical density at 600 nm (OD_{600}) after 24 h of incubation with tartrazine (0–3000 µg/mL) at 37 °C and expressed as a percentage of the untreated control. The OD_{600} measurements were confirmed by colony-forming unit (CFU) enumeration. Data are presented as the mean ± SD of three independent experiments (n = 3). Statistical analysis was performed using one-way ANOVA followed by Dunnett's multiple comparison test versus the untreated control. *E. coli*: $P < 0.01$ (333 and 1000 µg/mL), **$P < 0.0001$ (3000 µg/mL); *E. faecalis*: $P < 0.01$ (1000 µg/mL), **$P < 0.0001$ (3000 µg/mL); ns, not significant.